GENERATION OF SUB TERAHERTZ CHAOTIC RADIATION IN A HIGH-CURRENT RELATIVISTIC GYROTRON IN THE FREQUENCY MULTIPLICATION MODE

© 2025 N. S. Ginzburg[a], I. V. Zotova[a], A. N. Leontyev[a,b,*], A. M. Malkin[a], R. M. Rozental[a,b], A. S. Sergeev[a]

[a]Federal Research Center A.V. Gaponov-Grekhov Institute of Applied Physics of the Russian Academy of Sciences, Nizhny Novgorod, Russia

[b]National Research Lobachevsky State University of Nizhny Novgorod, Nizhny Novgorod, Russia

**e-mail: leontiev@ipfran.ru*

Received September 06, 2024

Revised September 16, 2024

Accepted September 30, 2024

Abstract. It is shown that for a high-current relativistic Ka-band gyrotron operating in the chaotic generation mode on the lowest mode of a circular waveguide $TE_{1,1}$, effective radiation is possible at the seventh harmonic of the gyrofrequency on the $TE_{7,2}$ mode. The relative width of the spectrum of chaotic sub terahertz radiation can exceed 5% at a megawatt output power level.

Keywords: *relativistic gyrotron, terahertz radiation, noise generation*

DOI: 10.31857/S03676765250115e6

INTRODUCTION

In the subterahertz and terahertz frequency range, the most powerful sources of monochromatic radiation are gyrotrons based on energy extraction from helical electron streams moving in vacuum. To date, continuous sources of radiation in the

range of 0.5 THz with an output power of 250 W have been realized [1], and in pulsed mode in the range of 0.67 THz with an output power of 200 kW [2] and in the range of 1 THz with an output power of 1-1.5 kW [3,4]. At the same time, gyrotrons also exhibit complex chaotic dynamics developing under conditions of large supercriticality (excess of operating current over the starting value). Thus, it was shown in [5,6] that under certain conditions gyrotrons can realize modes of generation of noise-like radiation with relative spectrum width up to 10%. The results of these studies were experimentally confirmed in [7], where Ka-band radiation with a relative spectrum width of 1.5% was obtained, which exceeded the values obtained in previous experimental works [8-10] by an order of magnitude. In turn, the possibility of creating a powerful source of broadband chaotic radiation based on high-current electron flux was discussed in [11]. According to estimates, the spectrum width of such a source in the Ka-band can exceed 30 GHz.

At the same time, it is of considerable interest to increase the frequency of the sources of chaotic radiation, which requires an increase in the value of the resonant magnetic field. The task at hand can be simplified by using the interaction at the harmonics of the gyrofrequency. This allows to reduce the operating value of the magnetic field proportional to the harmonic number. But selective excitation of chaotic oscillations on gyrofrequency harmonics is prevented by parasitic excitation of oscillations on the main harmonic.

In this connection, the use of the frequency multiplication effect in gyrotrons is of interest. The multiplication effect was first theoretically investigated in [12], where it was shown that the maximum radiation power at the second harmonic can be up to

several percent of the radiation power at the main harmonic. Subsequently, simultaneous emission at the second, third, and fourth harmonics in a gyrotron with an operating frequency of 0.13 THz was recorded in specially designed experiments [13]. However, until recently, such modes did not arouse significant interest. The situation changed with the publication of [14,15], where experimental measurements of the power level at the second harmonic of the gyrotron frequency in the range of 0.5 THz were made by filtering the low-frequency radiation. It was shown that the intensity ratio of the second harmonic to the first harmonic is in the range of 10^{-4}-10^{-3}, and the maximum power in the 0.52 THz range is close to 10 mW. Subsequently, the radiation from this gyrotron was used for spectral measurements by radioacoustic detection in the ranges 0.53, 0.79, and 1.06 THz, corresponding to the generation of radiation at the 2nd, 3rd, and 4th harmonics of the gyrofrequency [16].

In a recent work [17], the generation of chaotic radiation at the second harmonic of the gyrofrequency in a weakly relativistic gyrotron was studied for the first time. It was shown that it is possible to generate 0.5 THz radiation with a spectrum width of about 20 GHz and a power level of about 0.5 mW.

This work is devoted to analyzing the possibilities of obtaining broadband noise-like subterahertz radiation in a high-current gyrotron in the frequency multiplication mode.

MODEL AND BASIC EQUATIONS

Already in the first theoretical works, in which the unsteady dynamics of gyrotrons at the main cyclotron harmonic was considered, it was shown that a

significant increase of the current parameter is necessary for the transition to unsteady generation modes [18]:

$$I_0 = 16\frac{eJ_b}{mc^3}\cdot G\cdot\frac{\beta_{||}}{\beta_{\perp}{}^6} \quad (1)$$

where $J_b$is the electron beam current, m,e are the mass and charge of the electron, G is the coupling factor of the beam with the working mode, $\beta_{||}$, $\beta_{\perp}$ are the initial longitudinal and transverse velocities of electrons normalized to the speed of light c. In this case, to obtain modes of broadband chaotic generation, the value of the current parameter should be $I_0 \geq 1$. For high-current electron flows, this relation is quite easily provided by interaction with the lowest mode of the electrodynamic system $TE_{1,1}$.

It is known that for effective multiplication of radiation into a harmonic with number s, two conditions must be fulfilled [19,20]. If the gyrotron at the main cyclotron harmonic is excited at the $TE_{(m)\,(,)\,(n)}$mode, then the azimuthal index M of the mode at the *s-th* harmonic must satisfy the relation:

$$M = s\cdot \mathrm{m}. \quad (2)$$

At the same time, the condition of multiplicity of critical frequencies must be met,

$$\Omega_c = s\cdot \omega_c, \quad (3)$$

which it is convenient to rewrite for the values of the eigennumbers of the modes:

$$\nu_M = \frac{R_0\Omega_c}{c} = s\times\nu_m = s\frac{R_0\omega_c}{c} \quad (4)$$

where $R_0$is the radius of the homogeneous section of the gyrotron resonator.

Gyrotrons traditionally use resonators in the form of a segment of a cylindrical waveguide of circular cross section, the spectrum of modes of which is non-equidistant,

due to which the simultaneous exact fulfillment of conditions (2) and (4) is impossible. However, the above conditions are satisfied quite precisely for the combination of the $TE_{1,1}$mode at the main cyclotron harmonic and the $TE_{7,2}$mode at the seventh cyclotron harmonic.

Let us consider a model of a gyrotron in the form of a segment of a weakly irregular cylindrical waveguide of radius R_0, in which a helical electron beam excites $TE_{1,1}$at the main cyclotron harmonic and a mode $TE_{7,2}$at the seventh cyclotron harmonic. We will assume that the frequency of radiation at the first harmonic is close both to the critical frequency of the mode in the resonator $\overline{\omega}_1^{\,c}$, and to the cyclotron frequency $\omega_H = eH_0/m_e c\gamma_{(0)}$, where $H_0$is the magnitude of the leading magnetic field. In turn, the frequency of radiation at the seventh harmonic is close to the critical frequency of the second mode $\overline{\omega}_7^{\,c}$ and to seven times the cyclotron frequency $7\omega_H$. The electric field of each mode in the workspace can be represented as

$$\begin{aligned} \vec{E}_1 &= \mathrm{Re}\left(A_1(z,t)\,\vec{E}_\perp^{\,1}(r)\exp\left[i\omega_H t - i\varphi\right]\right) \\ \vec{E}_7 &= \mathrm{Re}\left(A_7(z,t)\,\vec{E}_\perp^{\,7}(r)\exp\left[7\left(i\omega_H t - i\varphi\right)\right]\right) \end{aligned} \qquad (5)$$

where $A_{(1,7)}(z,t)$ are slowly varying complex wave amplitudes at the first and second harmonic, respectively, the functions $\vec{E}_\perp^{\,1,7}(r)$ describe the radial structure of the modes, φ is the azimuthal angle. The electron-wave interaction can be described by the following system of equations:

$$
\begin{aligned}
&i\frac{\partial^2 a_1}{\partial Z^2}+\frac{\partial a_1}{\partial \tau}+\left(i\Delta_1+i\delta_1\left(Z\right)+\sigma_1\right)a_1=i\frac{I_1}{4\pi^2}\int_0^{2\pi}\int_0^{2\pi}pd\varphi d\theta_0\\
&i\frac{\partial^2 a_7}{\partial Z^2}+\frac{\partial a_7}{\partial \tau}+\left(i\Delta_7+i\delta_7\left(Z\right)+\sigma_7\right)a_7=i\frac{I_7}{4\pi^2}\int_0^{2\pi}\int_0^{2\pi}p^7 d\varphi d\theta_0\\
&\frac{\partial p}{\partial Z}+\frac{g^2}{4}\frac{\partial p}{\partial \tau}+ip\left(\left|p\right|^2-\left|p_0\right|^2\right)=i\left(a_1+a_7\left(p^*\right)^6\right)
\end{aligned}
\qquad (6)
$$

where $a_1=\frac{eA_1J_0\left(\nu_{11}R_b/R_0\right)}{mc\omega_H}\frac{1}{\gamma_0\beta_\perp^3}$ $a_7=\frac{eA_2J_0\left(\nu_{72}R_b/R_0\right)}{mc\omega_H}\frac{\beta_\perp^3}{\gamma_0}$ are normalized wave amplitudes, $Z=\frac{\beta_\perp^2}{2\beta_\parallel}\frac{\omega_H}{c}z$ $\tau=\frac{\beta_\perp^4}{8\beta_\parallel^2}\omega_H t$ are longitudinal coordinate and time, and p is the complex transverse pulse normalized to the initial value,

$$
\begin{aligned}
&\Delta_1=8\frac{\beta_{\parallel 0}^2}{\beta_{\perp 0}^4}\frac{\omega_H-\bar{\omega}_1^c}{\bar{\omega}_1^c},\ \Delta_7=392\frac{\beta_{\parallel 0}^2}{\beta_{\perp 0}^4}\frac{7\omega_H-\bar{\omega}_7^c}{\bar{\omega}_7^c}\\
&\delta_1\left(Z\right)=8\frac{\beta_{\parallel 0}^2}{\beta_{\perp 0}^4}\frac{\bar{\omega}_1^c-\omega_1^c\left(Z\right)}{\bar{\omega}_1^c},\ \delta_7\left(Z\right)=392\frac{\beta_{\parallel 0}^2}{\beta_{\perp 0}^4}\frac{\bar{\omega}_7^c-\omega_7^c\left(Z\right)}{\bar{\omega}_7^c}
\end{aligned}
\qquad (7)
$$

cyclotron and geometric detuning, $\omega_1^c(Z)=\nu_{11}c/R(z)$, $\omega_7^c(Z)=\nu_{72}c/R(z)$ – functions specifying the dependences of the critical mode frequencies on the longitudinal coordinate,

$$
\begin{aligned}
&I_1=16\frac{eI_b}{m_ec^3}\frac{\beta_\parallel}{\gamma_0\beta_\perp^6}\frac{J_0^2\left(\nu_{11}R_b/R_0\right)}{\left(\nu_{11}^2-1\right)J_1^2\left(\nu_{11}\right)}\\
&I_2=64s^3\left(\frac{s^s}{2^s s!}\right)^2\frac{eI_b}{m_ec^3}\frac{\beta_\parallel\beta_\perp^6}{\gamma_0}\frac{J_0^2\left(\nu_{72}R_b/R_0\right)}{\left(\nu_{72}^2-s^2\right)J_7^2\left(\nu_{72}\right)}
\end{aligned}
\qquad (8)
$$

- excitation parameters for a beam with injection radius $R_b$and current I_b, ν_{11}, $\nu_{72}$are the first and second roots of equations $J_1'(\nu)=0$ and $J_7'(\nu)=0$, respectively, s= 7 is the number of the cyclotron harmonic, on which the interaction with the second mode takes

place, $\sigma_1=4\beta_{||}^2/Q_1\ \beta_\perp^4$, $\sigma_7=196\beta_{||}^2/Q_7\ \beta_\perp^4$- absorption coefficients, $Q_{1,7}$- ohmic modes goodness of fit.

We will assume that at the entrance to the interaction space the electrons are uniformly distributed along the cyclotron rotation phases $p(Z=0)=\exp(i\theta_{(0)})$, $\theta_{(0)}=[0,2\pi)$. Reflection-free boundary conditions on the left and right boundaries of the system are used for the amplitudes of each mode:

$$\begin{aligned}
&a_1(\tau,0)-\frac{1}{\sqrt{i\pi}}\int_0^\tau \frac{e^{-i\left(\delta_1(0)+\Delta_1-i\sigma_1\right)(\tau-\tau')}}{\sqrt{\tau-\tau'}}\frac{\partial a_1(\tau',0)}{\partial Z}d\tau'=0,\\
&a_7(\tau,0)-\frac{1}{\sqrt{2i\pi}}\int_0^\tau \frac{e^{-i\left(\delta_7(0)+\Delta_7-i\sigma_7\right)(\tau-\tau')}}{\sqrt{\tau-\tau'}}\frac{\partial a_7(\tau',0)}{\partial Z}d\tau'=0,\\
&a_1(\tau,L)+\frac{1}{\sqrt{i\pi}}\int_0^\tau \frac{e^{-i\left(\delta_1(L)+\Delta_1-i\sigma_1\right)(\tau-\tau')}}{\sqrt{\tau-\tau'}}\frac{\partial a_1(\tau',L)}{\partial Z}d\tau'=0,\\
&a_7(\tau,L)+\frac{1}{\sqrt{2i\pi}}\int_0^\tau \frac{e^{-i\left(\delta_7(L)+\Delta_7-i\sigma_7\right)(\tau-\tau')}}{\sqrt{\tau-\tau'}}\frac{\partial a_7(\tau',L)}{\partial Z}d\tau'=0.
\end{aligned} \tag{9}$$

where L is the normalized length of the interaction space.

MODELING RESULTS

We further investigate the dynamics of a Ka-band high-current gyrotron with a $TE_{1,1}$working mode at the first harmonic of the gyrofrequency excited by a helical electron beam with an energy of 500 keV, a current of 0.5 kA, and a pitch factor of 1.0. For the above parameters, the value of the current parameter at the first cyclotron harmonic is about 3.5.

Fig. 1 shows the dependences of the average generation power and the spectrum width at the first and seventh cyclotron harmonics of the gyrofrequency when the magnetic field is changed. The spectrum width was calculated at the level of -10 dB relative to the maximum spectrum level. When the magnetic field is increased from 20

to 26 kE, the average generation power at the first harmonic decreases from a level of about 8 MW to 1 MW. At the same time, the average spectrum width increases from values of the order of 1 GHz to values of the order of 10-15 GHz.

In turn, a somewhat different picture is observed at the seventh cyclotron harmonic. The emission spectrum is concentrated in the range of more than 240 GHz (Fig. 2). The average generation power at increasing the magnetic field from 20 to 26 kE increases from values at the level of hundreds of kilowatts to the level of 1-2 MW. The power level of more than 1 MW is reached at a magnetic field of about 22 kE. In turn, the width of the chaotic generation spectrum fluctuates relative to the 10 GHz level. When the magnetic field increases above 25 kE, the width of the spectrum decreases successively, with a spectrum bifurcation in the region of 26 kE magnetic field. Thus, the optimal range of magnetic fields is 22-25 kE, in which stable generation with an average power level of more than 1 MW is observed in the subterahertz range at a spectrum width of 10 and more GHz.

CONCLUSION

Recent experimental studies have confirmed the promising use of frequency multiplication modes in gyrotrons excited by high-current electron fluxes [21]. In such gyrotrons, the level of emission at gyrofrequency harmonics turns out to be significantly higher compared to systems with weakly relativistic electron beams. The study allows us to draw a similar conclusion for chaotic generation modes.

FUNDING

The study was supported by the Russian Science Foundation (project No. 23-12-00161).

REFERENCES

1. *Glyavin M.Y., Kuftin A.N., Morozkin M.V. et al.* // IEEE Electron Device Lett. 2021. V. 42. No. 11. P. 1666.

2. *Glyavin M.Yu., Luchinin A.G., Nusinovich G.S. et al. //* Appl. Phys. Phys. Lett. 2012. V. 101. P. 153503.

3. *Glyavin M.Yu., Luchinin A.G., Golubiatnikov G.Yu.* // Phys. Rev. Lett. 2008. V. 100. Art. No. 015101.

4. *Kalynov Yu.K., Bandurkin I.V., Osharin I.V. et al.* // IEEE Electron Dev. Lett. 2023. V. 44. No.10. P.1740.

5. *Ginzburg N.S., Rozental R.M., Sergeev A.S. et al.* // Phys. Rev. Lett. 2017. V. 119. Art. No. 034801.

6. *Rozental' R.M., Ginzburg N.S., Sergeev A.S. et al.* // Tech. Phys. 2017. V. 62. P. 1562.

7. *Rozental R.M., Fedotov A.E., Ginzburg N.S. et al.* // Tech. Phys. Lett. 2019. V. 45. P. 511.

8. *Chang T.H., Chen C.N., Barnett L.R., Chu K.R.* // Phys. Rev. Lett. 2001. V. 87. Art. No. 064802.

9. *Rozental R.M., Zaitsev N.I., Kulagin I.S. et al.* // IEEE Trans. Plasma Sci. 2004. V. 32. No. 2. P. 418.

10. *Alberti S., Ansermet J.-Ph., Avramides K.A. et al.* // Phys. Plasmas. 2012. V. 19. No. 12. Art. No. 123102.

11. *Rozental R.M., Leontyev A.N., Sergeev A.S. et al.* // Bull. Russ. Acad. Sci. Phys. 2020. V. 84. No. 2. P. 189.

12. *Zavol'skii N.A., Nusinovich G.S., Pavel'ev A.B.* // Radiophys Quantum Electron. 1988. V. 31. No. P. 269.

13. *Idehara T., Yamagishi Y., Tatsukawa T.* // Int. J. Infrared Millim. THz Waves. 1997. V. 18. P. 259.

14. *Rumyantsev V.V., Maremyanin K.V., Fokin A.P. et al.* // Semiconductors. 2019. V. 53. No. 9. P. 1217.

15. *Glyavin M., Zotova I., Rozental R. et al*. // Int. J. Infrared Millim. THz Waves. 2020. V. 41. P. 1245.

16. *Golubiatnikov G.Y., Koshelev M.A., Tsvetkov et al.* // IEEE Trans. Terahertz. Sci. Tech. 2020. V. 10. No. 5. P. 502.

17. *Rozental R.M., Ginzburg N.S., Malkin A.M. et al*. // Int. J. Infrared Millim. THz Waves. 2023. V. 44. No. 11-12. P. 924.

18. *Ginzburg N.S., Nusinovich G.S., Zavolsky N.A.* // Int. J. Electron. 1986. V. 61. P. 881.

19. *Denisov G.G., Zotova I.V., Malkin A.M. et al.* // Phys. Rev. E. 2022. V. 106. No. 2. Art. No. L023203.

20. *Denisov G., Zotova I., Zheleznov I. et al.* // Appl. Sciences. 2022. V. 12. Art. No. 11370.

21. *Abubakirov E.B., Denisenko A.N., Leontyev A.N., et al. et al.* // IEEE Trans.

Electron Dev. 2024. V. 71. No. 4. P. 2821

FIGURE CAPTIONS

Fig. 1. Dependence of the average generation power and spectrum width at the first and seventh cyclotron harmonics on the magnetic field value.

Fig. 2. Output emission spectra at the seventh cyclotron harmonic.

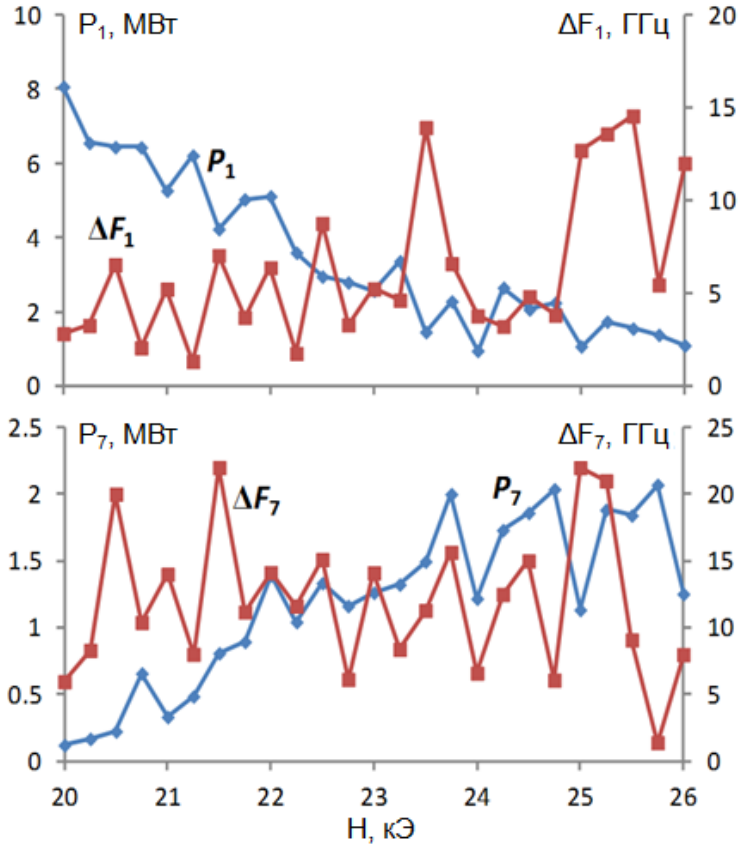

Fig. 1.

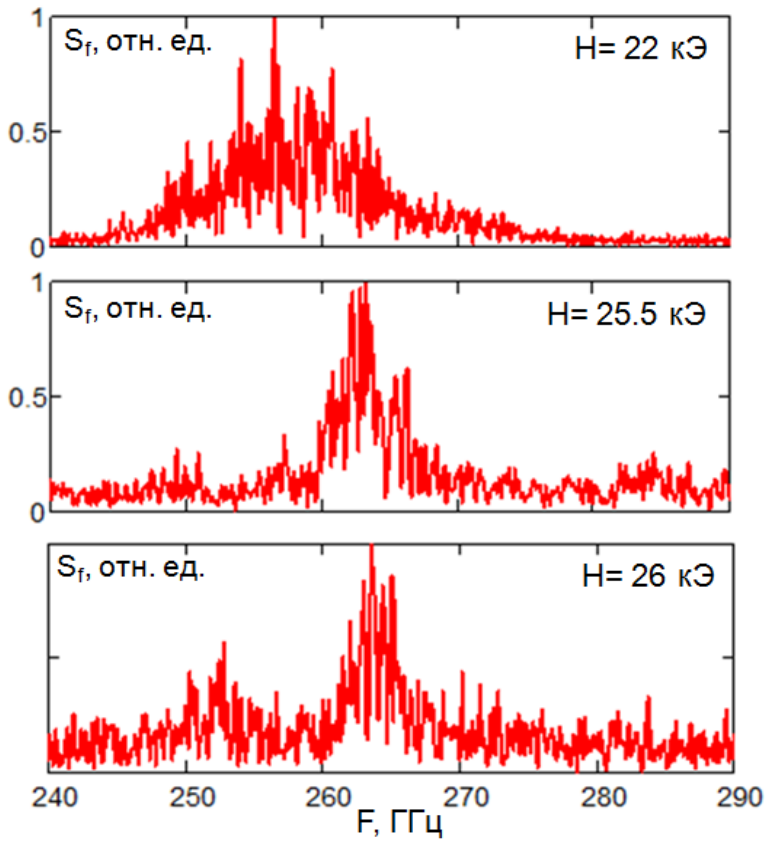
1
0.5
0
Sf, отн. ед.
H= 22 кЭ
1
0.5
0
Sf, отн. ед.
H= 25.5 кЭ
Sf, отн. ед.
H= 26 кЭ
240
250
260
270
280
290
F, ГГц

Fig. 2.